A Summary of "A Direct Transition State Theory Based Study of Methyl Radical Recombination Kinetics"

Stephen J. Klippenstein

Chemistry Department, Case Western Reserve University, Cleveland, Ohio 44106-7078

Lawrence B. Harding

Chemistry Division, Argonne National Laboratory, Argonne, Illinois, 60439

Received: January 10, 2000

Multireference configuration interaction based quantum chemical calculations are directly implemented in a variational transition state theory based analysis of the kinetics of methyl radical recombination. Separations ranging from 1.9 to 5.5 Å are considered for two separate forms for the reaction coordinate. The a priori prediction for the high-pressure limit rate constant gradually decreases with increasing temperature, with a net decrease of a factor of 1.7 from 300 to 1700 K. Near room temperature, this theoretical estimate is in quantitative agreement with the experimental data. At higher temperatures, comparison between theory and experiment requires a model for the pressure dependence. Master equation calculations employing the exponential down energy transfer model suggest that the theoretical and experimental high-pressure limits gradually diverge with increasing temperature, with the former being about 3 times greater than the latter at 1700 K. The comparison with experiment also suggests that the energy transfer coefficient, $<\Delta E_{down}>$, increases with increasing temperature.

Summary

The following is a brief summary of ref 1, which was intended to be published in this special issue honoring William A. Goddard, III. For complete details, see ref 1.

A direct, variational, transition state theory (TST) study of the methyl radical recombination reaction is reported employing high-level ab initio electronic structure calculations. This reaction is of considerable importance in combustion and has been the subject of numerous experimental[2−11] and theoretical studies.[7,12−33] The focus of this study is the high-pressure limiting rate constant as a function of temperature. To compare to experimental results (which for temperatures above 400 K are not at the high-pressure limit) we also report a one-dimensional, master equation treatment of the pressure dependence.

The methyl−methyl interaction potential was evaluated with multireference, configuration interaction (MR-CI) calculations, using both polarized double-ζ (cc-pvdz) and augmented polarized triple-ζ (aug-cc-pvtz) basis sets. A sample plot showing the calculated interaction energy for three different orientations as a function of the carbon−carbon distance is displayed in Figure 1. In the majority of the calculations the internal geometries of the two methyl fragments are kept fixed; however, the importance of allowing the two umbrella angles to relax has been explored. In Figure 2 we show a plot of the optimum umbrella angle as a function of the CC distance.

Neglecting the internal degrees of freedom of each methyl radical leaves a total of six geometric degrees of freedom to be explored. These consist of the distance between the two radicals and five orientational degrees of freedom, corresponding to the five transitional modes of this reaction. To calculate the high-pressure limit rate constant one needs to evaluate the contribution to $N_{EJ}^{\dagger}$ (the transition state number of states) from these transitional modes. This is done using a classical phase space integral formalism. In this work, the transitional mode phase space integrals are evaluated at the energy, *E*, and total angular

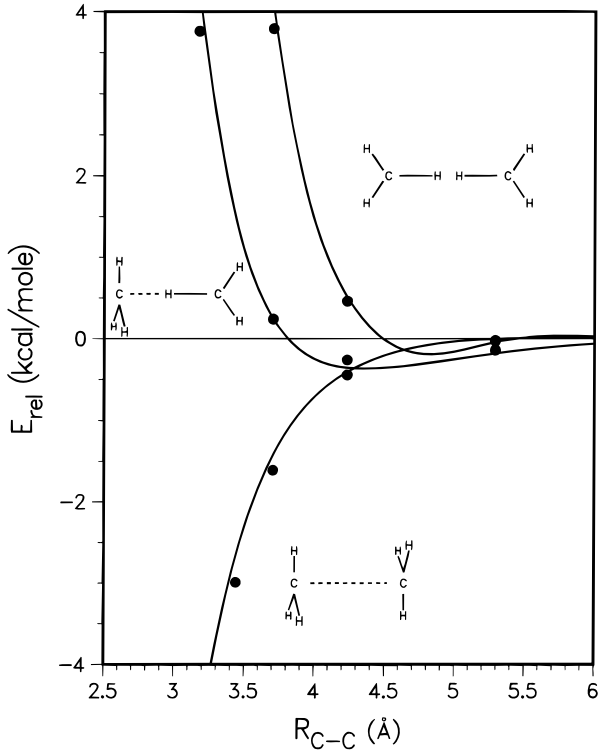

Figure 1. Plots of the energy as a function of the CC distance for three fixed orientations (as shown). The lines are the results of calculations using the cc-pvdz basis set. The solid circles denote results from aug-pvtz calculations. For all calculations the geometries of the two methyl fragments are kept frozen (planar).

10.1021/jp000120t CCC: $19.00
Published on Web 02/15/2000

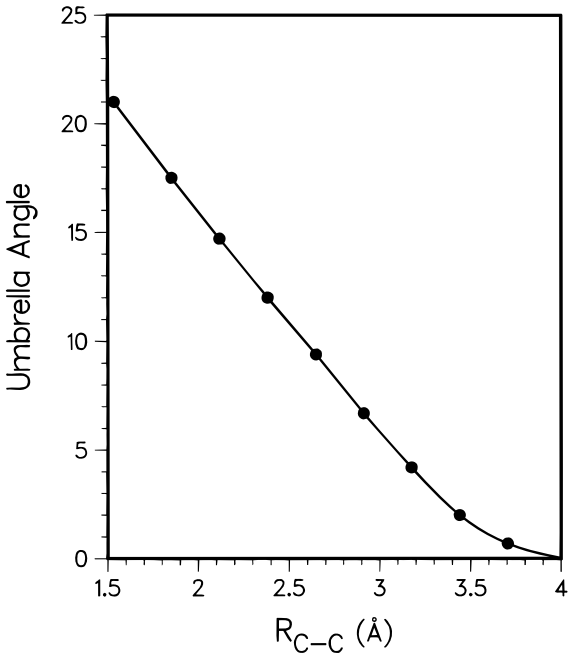

Figure 2. Optimum methyl umbrella angle as a function of the CC distance from CAS+1+2/cc-pvdz calculations. An angle of 0° corresponds to planar radicals. The molecule is constrained to be of D_{3d} symmetry.

momentum, *J*, resolved level. A crude Monte Carlo integration technique is employed in the evaluation of these phase space integrals, with the requisite potential energies determined directly from the MR-CI quantum chemical simulations. Two choices for pivot points (used to define the transition state dividing surface) were explored. Altogether a total of 14 600 geometrical configurations were sampled. Corrections were added to account for (a) the relaxation energy associated with allowing the methyl radical fragments to relax from a planar geometry, (b) changes in the vibrational frequencies of the conserved modes as the radicals approach, and (c) the use of the relatively small cc-pvdz basis set. The final, high-pressure limiting rate constants are plotted in Figure 3.

As noted above the, experimental studies have been unable to reach the high-pressure limit for temperatures above 400 K. Modeling of the pressure dependence is therefore required for comparisons between theory and experiment at temperatures above 400 K. At finite pressures, below the high-pressure limit, the effective bimolecular rate constant for methyl radical recombination corresponds to a thermal average of the initial rate of formation of energized ethane complexes, at each energy, *E*, and total angular momentum, *J*, times the probability of collisional stabilization at each *E* and *J*. Since a single collision does not always yield a stabilized complex, the determination of the stabilization probability requires an analysis of the time dependence of the populations in each *E* and *J* state, as done in the master equation approach. In this work a one-dimensional form of the master equation is used in which the *J* dependence of the populations is averaged over. Sample plots of the low temperature, pressure dependence are shown in Figure 4. From this plot it can be seen that quantitative agreement between theory and experiment is obtained for values of the energy transfer coefficients, $<\Delta E_{down}>$ in the range 100 to 200 cm^{-1}.

In Figure 5, we show a sample plot of the pressure dependence at a higher temperature (577 K). The upper plot

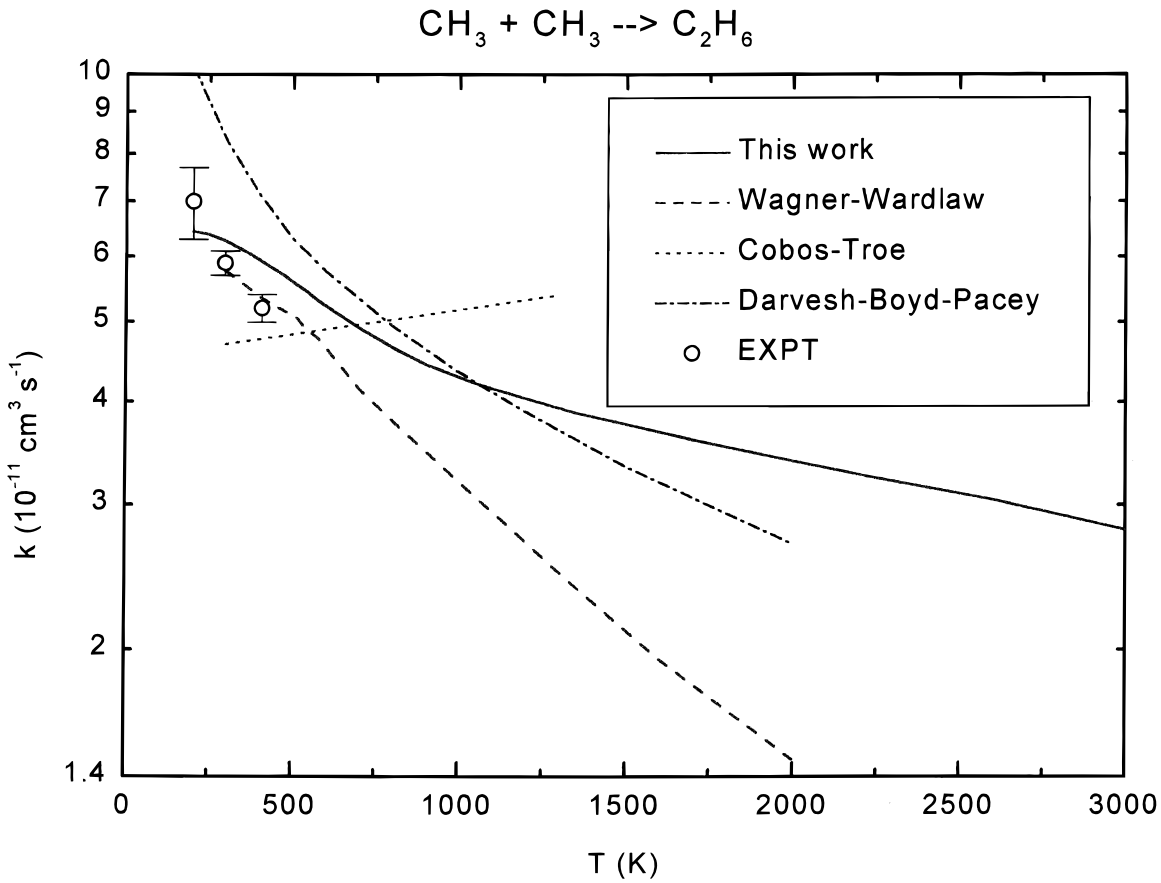

Figure 3. Plot of the temperature dependence of the high-pressure limiting rate constant for methyl radical association. The solid, dashed, and dashed−dotted lines represent the TST calculations from this work, from ref 19, and from ref 21, respectively. The dotted line denotes the SACM calculations from ref 14. The circles denote the experimental results from refs 5−7.

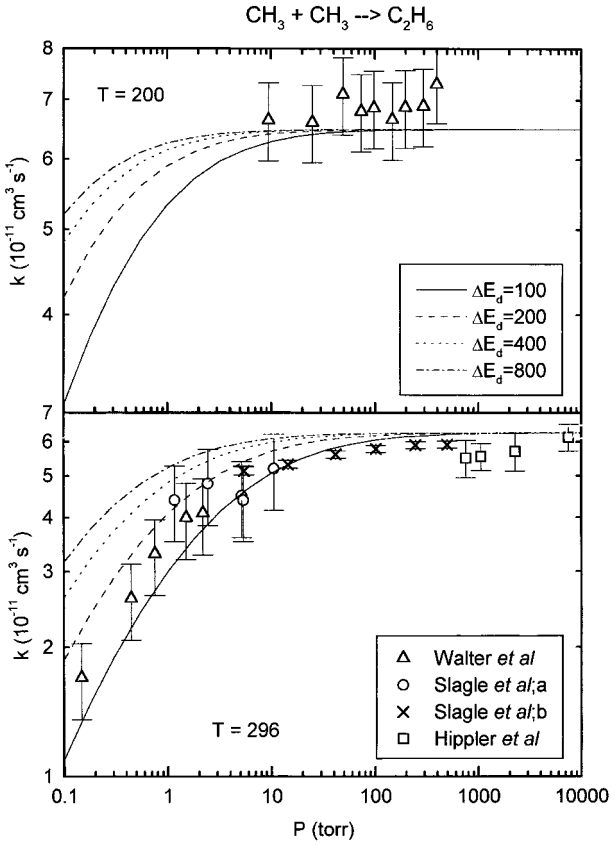

Figure 4. Plots of the pressure dependence of the rate constant for temperatures of 200 and 296 K. The squares denote the experimental data of Hippler et al.,[5] the circles and crosses of Slagle et al.,[6] and the triangles of Walter et al.[7] The lines denote the present theoretical results for various $<\Delta E_{down}>$ values.

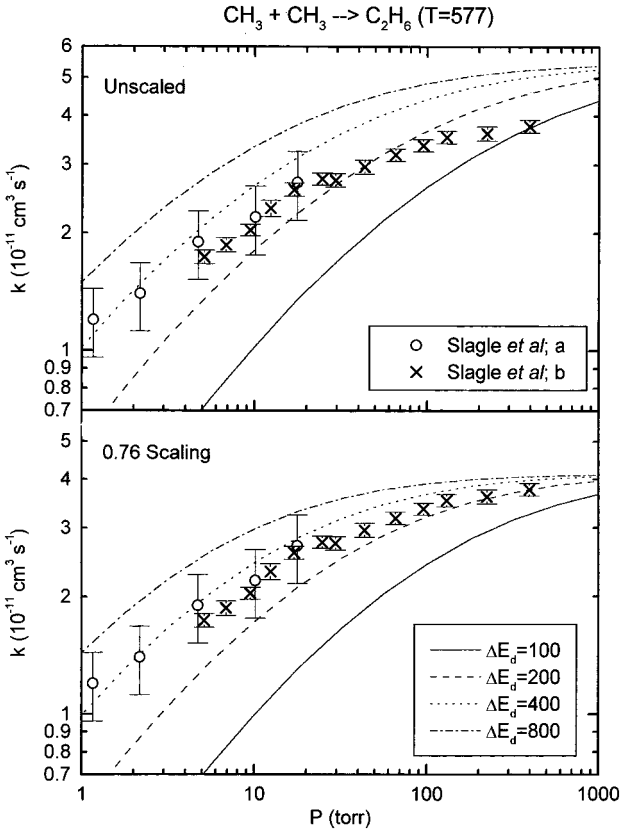

Figure 5. As in Figure 4, but for a temperature of 577 K. The theoretical results in the lower plot employ a transition state number of states which are scaled to yield a high-pressure thermal rate constant which is 0.76 times as large as the unscaled result. The upper plot provides the unscaled theoretical results.

shows the unadjusted theoretical predictions, which appear to be converging to a high-pressure limit above that of the experiment. The lower plot shows theoretical results in which the high-pressure limit has been scaled by a factor of 0.76 using an energy dependent scaling of the transition state number of states. Using either the scaled or unscaled results, optimum agreement between theory and experiment is obtained for $<\Delta E_{down}>$ values of range 200 to 400 cm^{-1}. Similar and greater deviations between unscaled theoretical results and pressure dependent experimental results persist to temperatures of 1700 K.

The primary conclusions from this work are as follows:

(1) The ability to do direct dynamical calculations using accurate, ab initio, MR-CI calculations has been demonstrated.

(2) The calculations present strong evidence for a decrease in $k_\infty(T)$ with increasing temperature (the total predicted change amounts to a decrease by a factor of 1.7 between 300 and 1700 K). The increasing hindrance of the transitional modes at shorter distances is the dominant factor in this decreasing rate.

(3) The conserved modes have two competing effects on the temperature dependence. The relaxation energy (arising from the geometric relaxation of the internal coordinates of the methyl radicals) increases the rate constant by a factor of 2.2 between 300 and 1700 K. The increasing stiffness of the conserved mode vibrational frequencies, as the separation between the two fragments decreases, decreases the recombination rate by a factor of 1.3 in this same temperature range. The umbrella modes are the dominant components in both of these variations. The net effect of the conserved mode variations corresponds to an increase in the rate constant by a factor of 1.7 from 300 to 1700 K. As noted above this is more than offset by the increasing hindrance of the transitional modes.

(4) There is excellent agreement between the present theoretical, room temperature, recombination rate and previous experimental results. At higher temperatures, however, the theoretical and experimental results become increasingly discordant, with the experimental results appearing to extrapolate to a high-pressure limit that is lower than that obtained from the theory. These discrepancies may be indicative of either a failure in the model for the pressure dependence or an overestimate of $k_\infty(T)$ at higher temperatures. One possible explanation for this difference is that a fraction of the trajectories may be directly repulsive (i.e., trajectories that come in to small separations but then immediately turn around and dissociate back to reactants) and that this fraction increases with increasing temperature.

(5) Comparisons between theory and experiment suggest that the energy transfer coefficient, $<\Delta E_{down}>$, increases with increasing temperature.

Acknowledgment. This work was supported by the U.S. Department of Energy, Office of Basic Energy Sciences, Division of Chemical Sciences, under Contract W-31-109-ENG-38 (L.B.H. and S.J.K.) and through NSF grant CHE-9423725 (S.J.K.).

Noted Added in Proof: It has come to our attention that refs 34 and 35 provide the earliest variational transition state theory studies of the $CH_3 + CH_3$ reaction (and indeed of any barrierless reaction). In contrast with the present study, ref 35 predicts a rise in the rate constant with increasing temperature, perhaps due to the empirical assumptions for the form of the potential in the transition state region.

It is also worth noting that, for the $CH_3 + H$ and $Cl^- + CH_3Cl$ reactions, variational transition state theory calculations employing a rigid vibrator reaction path Hamiltonian approach (which is relatively simple to implement) are in good agreement with phase space integral based treatments analogous to the present one.[36−39] Furthermore, for H + diamond the reaction path treatment yields good agreement with trajectory results.[40] However, in other cases, (e.g., $CH_2 + CO$, H + CCH, $CF_3 +$ H, and $CH + H_2$[41,42]) there are significant discrepancies between calculations employing a purely quadratic transitional mode potential and the full potential. Some of these discrepancies may be related to the coupling of conserved and transitional modes, which are neglected in the phase space integral treatment. However, the reasonably large separations for the transition state, and the generally small variations in conserved mode force fields at such separations, suggest that the effect of such couplings is minimal.

In general, the validity of the rigid vibrator reaction path Hamiltonian approach depends primarily on the suitability of the quadratic representation of the transitional mode potential, which should at least qualitatively correlate with the heights of the barriers for the transitional modes.[43] Notably, if neither of the reactants is an atom, then at least one of the transitional mode motions corresponds to a torsional motion. The generally small barriers for such torsional motions then yield considerable uncertainty in a purely quadratic potential based result. To bypass this problem, one may introduce separable anharmonic treatments for some of the modes, as was successfully done, for example, in ref 44 for $H + O_2$ with total angular momentum $J = 0$. However, the large amplitude of the motion experienced for the torsional mode(s) may lead to significant transitional mode coupling effects, particularly for non-zero J.

References and Notes

(1) Klippenstein, S. J.; Harding, L. B. *J. Phys. Chem.* **1999**, *103*, 9388.
(2) Mallard, W. G. NIST Chemical Kinetics Database, 1992, and references therein.
(3) Glänzer, K.; Quack, M.; Troe, J. *Chem. Phys. Lett.* **1976**, 39, 304.
(4) Glänzer, K.; Quack, M. Troe, J. In *Sixteenth Symposium (International) Combustion*; The Combustion Institute: Pittsburgh, PA, 1977; p 949.
(5) Hippler, H.; Luther, K.; Ravishankara, A. R.; Troe, J. *Z. Phys. Chem. NF* **1984**, *142*, 1.
(6) Slagle, I. R.; Gutman, D.; Davies, J. W.; Pilling, M. J. *J. Phys. Chem.* **1988**, *92*, 2455.
(7) Walter, D.; Grotheer, H.-H.; Davies, J. W.; Pilling, M. J.; Wagner, A. F. In *Twenty-Third Symposium (International) Combustion*; The Combustion Institute, Pittsburgh, PA, 1990; p 107.
(8) Hwang, S. M.; Wagner, H. G.; Wolff, T. *In Twenty-Third Symposium (International) Combustion*; The Combustion Institute: Pittsburgh, PA, 1990; p 99.
(9) Hwang, S. M.; Rabinowitz, M. J.; Gardiner, W. C., Jr. *Chem. Phys. Lett.* **1993**, *205*, 157.
(10) Davidson, D. F.; DiRosa, M. D.; Chang, E. J.; Hanson, R. K.; Bowman, C. T. *Int. J. Chem. Kinet.* **1995**, *27*, 1179.
(11) Du, H.; Hessler, J. P.; Ogren, P. J. *J. Phys. Chem.* **1996**, *100*, 974.
(12) Gorin, E. J. *J. Chem. Phys.* **1939**, *7*, 256.
(13) Quack, M.; Troe, J. *Ber. Bunsen-Ges. Phys. Chem.* **1977**, *81*, 329.
(14) Cobos, C. J.; Troe, J. *J. Chem. Phys.* **1985**, *83*, 1010.
(15) Wardlaw, D. M.; Marcus, R. A. *J. Chem. Phys.* **1985**, *83*, 3462.
(16) Wardlaw, D. M.; Marcus, R. A. *J. Phys. Chem.* **1986**, *90*, 5383.
(17) Evleth, E. M.; Kassab, E. *Chem. Phys. Lett.* **1986**, *131*, 475.
(18) Klippenstein, S. J.; Marcus, R. A. *J. Chem. Phys.* **1987**, *87*, 3410.
(19) Wagner, A. F.; Wardlaw, D. M. *J. Phys. Chem.* **1988**, *92*, 2462.
(20) Smith, S. C.; Gilbert, R. G. *Int. J. Chem. Kinet.* **1988**, *20*, 307.
(21) Darvesh, K. V.; Boyd, R. J.; Pacey, P. D. *J. Phys. Chem.* **1989**, *93*, 4772.
(22) Stewart, P. H.; Larson, C. W.; Golden, D. M. *Combust. Flame* **1989**, *75*, 25.
(23) Aubanel, E. E.; Roberston, S. H.; Wardlaw, D. M. *J. Chem. Soc., Faraday Trans.* **1991**, *87*, 2291.
(24) Forst, W. *J. Phys. Chem.* **1991**, *95*, 3612.
(25) Roberston, S. H.; Wardlaw, D. M.; Hirst, D. M. *J. Chem. Phys.* **1993**, *99*, 7748.
(26) Pitt, I. G.; Gilbert, R. G.; Ryan, K. R. *J. Phys. Chem.* **1995**, *99*, 239.
(27) Robertson, S. H.; Pilling, M. J.; Baulch, D. L.; Green, N. J. B. *J. Phys. Chem.* **1995**, *99*, 13452.
(28) Hessler, J. P.; Ogren, P. J. *J. Phys. Chem.* **1996**, *100*, 984.
(29) Hessler, J. P. *J. Phys. Chem.* **1996**, *100*, 2141.
(30) Jeffrey, S. J.; Gates, K. E.; Smith, S. C. *J. Phys. Chem.* **1996**, *100*, 7090.
(31) Pesa, M.; Pilling, M. J.; Robertson, S. H.; Wardlaw, D. M. *J. Phys. Chem. A* **1998**, *102*, 8526.
(32) Pacey, P. D. *J. Phys. Chem. A* **1998**, *102*, 8541.
(33) Naroznik, M. *J. Chem. Soc., Faraday Trans.* **1998**, *94*, 2531.
(34) Hase, W. L. *J. Chem. Phys.* **1972**, *57*, 730.
(35) Hase, W. L. *J. Chem. Phys.* **1976**, *64*, 2442.
(36) Hase, W. L.; Mondro, S. L.; Duchovic, R. J.; Hirst, D. M. *J. Am. Chem. Soc.* **1987**, *109*, 2916.
(37) Robertson, S. H.; Wagner, A. F.; Wardlaw, D. M. *J. Chem. Phys.* **1995**, *103*, 2917.
(38) Vande Linde, S. R.; Hase, W. L. *J. Phys. Chem.* **1990**, *94*, 2778.
(39) Klippenstein, S. J.; unpublished results.
(40) Song, K. Y.; De Sainte Claire, P.; Hase, W. L.; Hass, K. C. *Phys. Rev. B* **1995**, *52*, 2949. De Sainte Claire, P.; Barbarat, P.; Hase, W. L. *J. Chem. Phys.* **1994**, *101*, 2476.
(41) Klippenstein, S. J.; East, A. L. L.; Allen, W. D. *J. Chem. Phys.* **1996**, *105*, 118.
(42) Wagner, A. F.; Harding, L. B.; Robertson, S. H.; Wardlaw, D. M. *Ber. Bunsen-Ges. Phys. Chem.* **1997**, *101*, 391.
(43) Hase, W. L., private communication.
(44) Song, K.; Peslherbe, G. H.; Hase, W. L.; Dobbyn, A. J.; Stumpf, M.; Schinke, R. *J. Chem. Phys.* **1995**, *103*, 8891.